engineering proceedings

MDPI

Proceeding Paper

Current Measurement and Fault Detection Based on the Non-Invasive Smart Internet of Things Technique †

Abhrodeep Chanda and Abhishek Gudipalli *

School of Electrical Engineering, Vellore Institute of Technology, Vellore 632014, Tamil Nadu, India; abhrodeepc07@gmail.com

* Correspondence: abhishek.g@vit.ac.in

† Presented at the International Conference on Recent Advances in Science and Engineering, Dubai, United Arab Emirates, 4–5 October 2023.

Abstract: Graphing the consumption of daily essentials like electricity and water is crucial for minimising waste and estimating per-user usage in light of the modern-day data acquisition rally for a better understanding of customer consumption and patterns. Traditional methods of electrical measurement require the involvement of a trained professional, while more advanced alternatives can be prohibitively expensive or offer limited customisation options. We address the cost factor, flexibility, and complexity issues by using a non-intrusive clamp current transformer around power lines to measure current, estimate power, and upload it to the cloud with proper statistical data. For domestic and industrial applications, the filtered and referenced outputs are read by a low-cost CPU (ultra-low power) equipped with Wi-Fi, an analog-to-digital converter, and Bluetooth capabilities, which then determines the apparent power with an accuracy of 0.37 to 0.8%. Nonlinearity varies from 0.2% to 0.3% as a function of increasing current; nonetheless, offsets are imperceptible under typical operating conditions. Safety in the event of a sudden, large change in the current profile is one of several factors that determine the current measuring limit, together with the rating of the current transformer utilised and other related filtering, reference, calibration, and coding criteria. Our goal is to make the power consumption statistics accessible on the move at little cost by simplifying the circuit and coding of traditional metres. It is smart in that no hard coding is required to send credentials across routers, and fault signals are detected and relayed in accordance with an algorithm. User-specific servers save data for monitoring and conserving energy usage; users do not need to consult specialists or put their own security at risk. Data are acquired from the power line and sent to the cloud where statistical functions are performed to increase insight into consumption and failure. It has impressive range and accuracy in terms of power and current for residential and business applications.

Keywords: current; cloud; fault detection; measurement; non-invasive; smart IoT

check for updates

Citation: Chanda, A.; Gudipalli, A. Current Measurement and Fault Detection Based on the Non-Invasive Smart Internet of Things Technique. *Eng. Proc.* **2023**, *59*, 174. https://doi.org/10.3390/engproc2023059174

Academic Editors: Nithesh Naik, Rajiv Selvam, Pavan Hiremath, Suhas Kowshik CS and Ritesh Ramakrishna Bhat

Published: 17 January 2024

Copyright: © 2024 by the authors. Licensee MDPI, Basel, Switzerland. This article is an open access article distributed under the terms and conditions of the Creative Commons Attribution (CC BY) license (https://creativecommons.org/licenses/by/4.0/).

1. Introduction

For the sake of future generations, it is incumbent upon the present generation to save energy and hence lower individual carbon footprints. To forecast future power needs and prevent either excess or deficiency, the power generation industry must collect and analyse massive amounts of data from a variety of sources, including homes, businesses, farms, and factories. The Prayas (Energy Group) 2014 survey [1], validated by the LBNL, MP ENsystems Pvt. Ltd. (Mumbai, India), and the IIASA, reports that out of India's total 2014 electricity consumption of 883 billion units, 22% went towards household use, 18% went towards agricultural use, 9% went towards commercial use, and went 44% towards industrial use. Figure 1 depicts the increase in selected states' home power consumption from 2004 to 2015 [2]. In 2014, the annual growth in the REC (rate of electricity consumption) was 8%. Extensive electrification in rural and urban India has led to a rise from 55% of homes having power in 2001 to 80% in 2017.

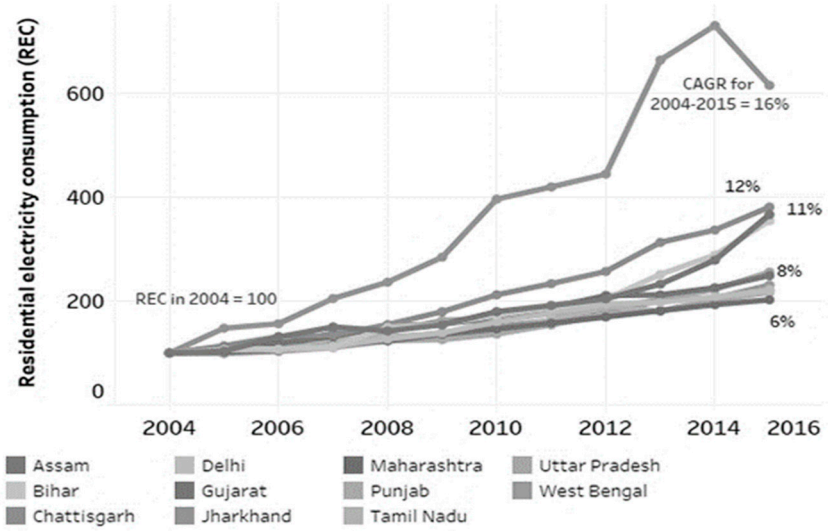


Figure 1. Residential electricity consumption growth in selected states (2004–2015) [2].

Power theft can be reduced, electricity consumption can be more accurately estimated, and power waste can be minimised with the use of low-cost, effective, and simple-to-deploy metering and submetering devices, as predicted by the rising demand trend. Flexible common metering panel boxes require intricate wiring for installation, and while they are reliable, their short lifespan can be attributed to the fact that they use electromagnetic technology and have moving parts. In the US and European countries, different contactless, non-invasive metering solutions are present like [3–7] Acme, Watts Up, WeMo Insight, TED, Magnetometer, Virtualization, Stick-on, and Monjolo, which are mostly plug types, split-core, magnetometers, current transformers, or piezo-electromagnetic, but the cost factor is much higher for them to be implemented on a large scale. We have zeroed in on the inductance current and ignored the voltage, except for its root-mean-square (RMS) value. This is a study of seeming power. The potential for contactless voltage measurement is considered promising for the device's long-term health [8]. The device achieves a constant voltage by combining average and mean square compensations at the household level. The 128 × 64 OLED display and the Wi-Fi module's transmission draw a combined 63–73 mA from the device's power supply, and an additional 100–116 mA is used when sending data to the cloud. The chip's deep-sleep feature can be utilised to drastically cut power consumption during periods of inactivity when the load is zero and a timer-wakeup or external wakeup signal is present. In the event of a power outage or device malfunction, the most recent readings can be retrieved from the onboard EEPROM or, failing that, the cloud. There is no need for rigid coding when it comes to delivering updates over-the-air (OTA). Meanwhile, the RMS value of current and apparent power is determined using a load bank with a current consumption range of 1–10 A. When compared to a standard with a resistive and inductive load, the measured current and apparent power show only minor deviations from the true values [9]. In order to even out the fluctuations, the programme uses mean estimates and root-mean-square estimations. As measured between 0 and 30 A, there is a 0.267%, or 0.08 A, discrepancy. Finally, we talk about the current and apparent power accuracy, which might vary between 2–2.5% and 0.05% from the actual measurement if the offset is not taken into account.

2. Related Works

Power measurement systems for industry and academia are produced in a vast variety. Costing a pretty penny and lacking convenient extras like wireless and cloud connectivity, today's split-core systems leave much to be desired. It is difficult and expensive to deploy plug-load with split-core devices with genuine power and actual power measurements

with phase angles, but the resulting algorithm for whole-line analysis is highly effective. It is possible to categorise the unseen parts as [10–14]:

1. Whole house meters;
2. Energy harvesting and non-harvesting;
3. Plug-load meters;
4. Non-contact meters.

The proposed design and method can help solve the complexity, expense, and employability problems that prevent more widespread use of this cutting-edge technology.

3. System Overview

Figure 2 depicts the device in its entirety. Clamper split-core designs like this one make it possible to measure the current passing through a line without cutting into it or otherwise disrupting the power supply [15–18]. Load refers to the entire house or medium-to-heavy appliances, which are notoriously difficult to equip with plug-load metres. By keeping tabs on energy consumption, you can evaluate defects remotely, reducing maintenance costs and extending the lifespan of your assets. The device can be used as an access point for any mobile device to connect to before it has been fully initialised. After entering the router or hotspot's SSID and password on the device's webpage, the device will begin reading the RMS current and uploading it to the cloud at regular intervals, as well as saving a copy of the hourly kWh reading to its EEPROM in case of a power outage. Just like a clamp metre, but with fewer electronics and more simplicity, a device based on the Internet of Things can be used independently of the cloud. Over-the-air updates are another option. With an over-the-air (OTA) patch, a device that has been calibrated and corrected for 230 V can be used with any other voltage. WPA, IEEE 802.11 b/g/n on the 2.4 GHz band, and the HTTP set of rules and protocols are used for the Wi-Fi signal. There is a range of 10 m for Wi-Fi. No energy harvesting mechanism is applied, thus a 3000 mAh battery is required for approx. 42 h of autonomy; nevertheless, direct power from the mains using an adapter is preferable [19–21].

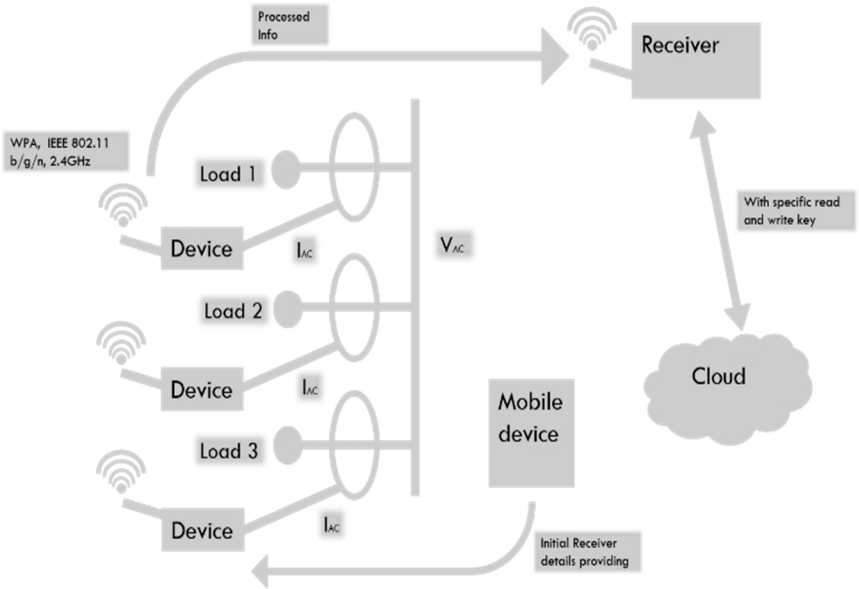


Figure 2. Device overview.

4. Design

The alternating voltage that comes out of the split-core current transformer has a peak value of about 1.414214 V (root mean square). The microcontroller (ESP32)'s logic

level [2] is divided in half to serve as a reference voltage because the ADC cannot convert the negative component:

$$(3.3/2 + 1.414214)\ \text{V} = 3.064214\ \text{V}$$

$$(3.3/2 - 1.414214)\ \text{V} = 0.235786\ \text{V}$$

which is within the limits of the ADC resolving capacity. A 12-bit, or 4096-bit, ADC is built in, and it operates at 3.3 V logic. This means that the greatest value is 3803 bits and the minimum value is 293 bits. Theoretically, 30 A/1 V as CT equates to a minimum resolving voltage of 810 V. Small range loads are eliminated to restrict the cost factor and simplify; however, accumulation as a residence/commercial building can be simply estimated, allowing for higher resolution. Figure 3 depicts the notion of a voltage divider/reference for reducing the negative value of the current created in the secondary of a split-core CT. An RC circuit with a 0.94-s time constant has been included for current curve smoothing. With the serial baud rate set to 115,200 bytes/s and the sampling rate set in code to 112 samples per 1 cycle, we obtain 5600 samples for every 50 cycles (ESP32 set for 5588 by the calcIrms function). Precision in adjusting the sampling rate also helps reduce offset by adding bias to the aforementioned linear equation.

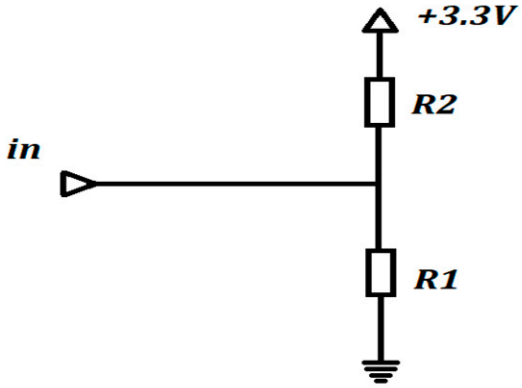


Figure 3. Linear relation between line current and ADC voltage referencing representation.

5. Implementation and Results

The numbers initially supplied by assessing the circuit in practical situations were more dependable and less prone to quick fluctuation after the weights/slope connected with the programming to the raw data arriving from CT secondary terminals were modified. The ADC's range is 0–3.3 V, which is 12-bit resolution (4096 bit), but due to the reference at 1.65 V, the highest to lowest is indicated as 3.1 V to 0.24 V. Using a trial-and-error approach, the weights in the Emon library can be combined to precisely adjust the calibration value for the raw data. Figure 4 shows the average daily current measured by cloud-based devices (beginning at night for a single room). As can be seen in Figure 5, when calculating the RMS value of the current, the reading can be off by as much as 2.5%. Device and ammeter values are presented for a 1–10 A load bank to demonstrate precision and sensitivity. While the secondary winding's accuracy improves with increasing current, the deviation increases as a result of the instantaneous current corresponding flux cutting. Figure 6 depicts the relationship between and among the various readings. Figure 7 shows that all of the readings are highly correlated, which indicates that they are entangled with one another and may be extrapolated to show that the device is functioning as expected and not giving random arbitrary values. Table 1 shows the actual vs. device readings.

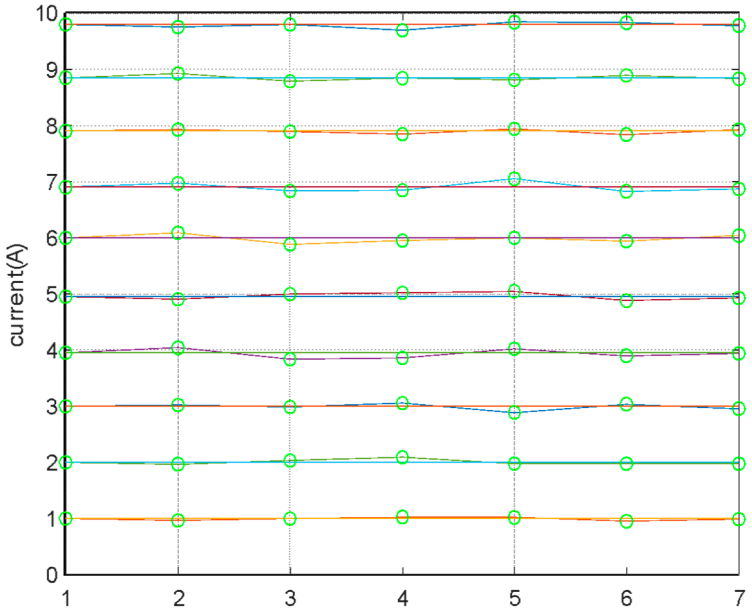


Figure 4. RMS current readings vs. the actual RMS current.

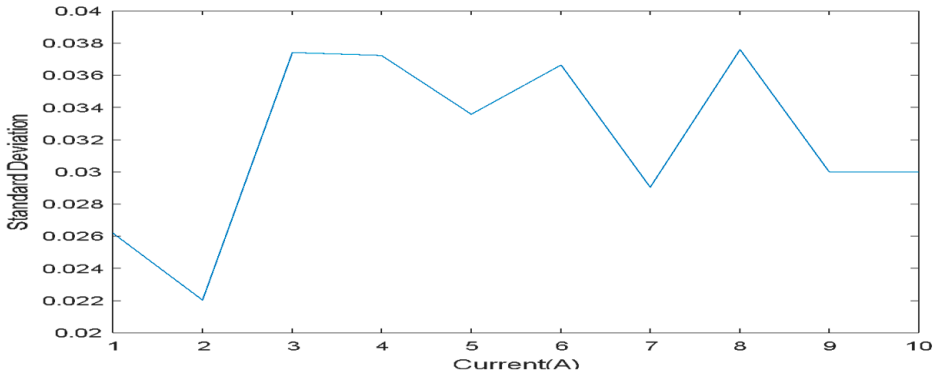


Figure 5. Standard deviation from the actual value of the current.

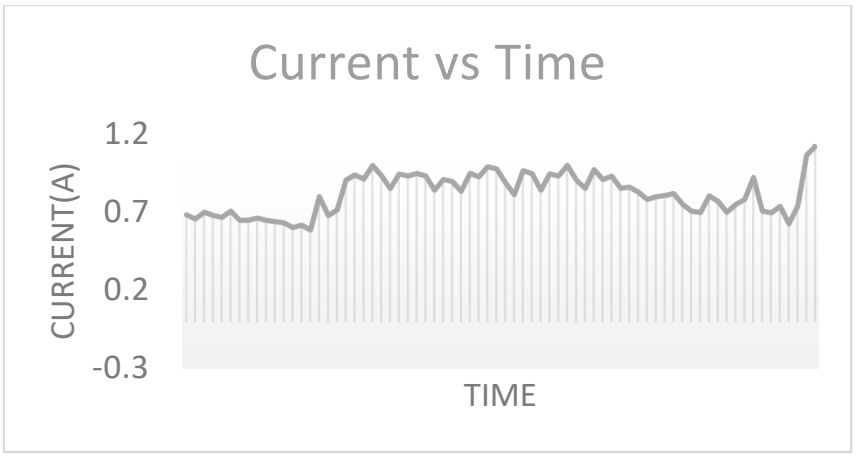


Figure 6. Current curve (RMS) for a day with device readings (starting from night for a single room) from cloud readings.

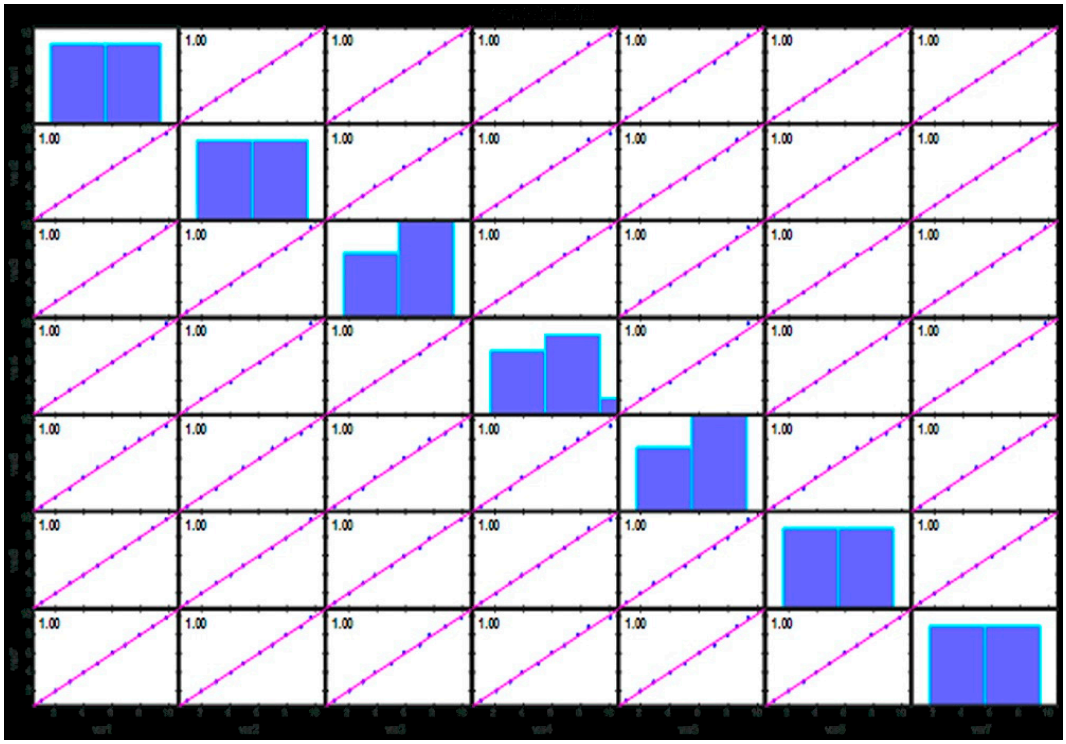


Figure 7. Correlation within and between each level reading.

Table 1. Actual vs. device readings (only a subset).

Actual (A)	Device Reading (A)					
1	0.97	1	1.03	1.02	0.95	0.99
2	1.97	2.04	2	1.98	1.99	1.98
3	3.02	2.99	3.06	2.95	3.04	2.96
3.95	4	3.89	3.92	3.94	3.9	3.94
4.95	4.91	4.94	5.02	4.98	4.95	4.93
6	5.99	5.96	5.95	6	5.94	6.04
6.9	6.93	6.89	6.88	6.84	6.9	6.87
7.9	7.93	7.88	7.85	7.94	7.84	7.93
8.85	8.9	8.86	8.84	8.81	8.89	8.83
9.8	9.75	9.8	9.77	9.84	9.83	9.78

6. Algorithm and Fault Detection

As mentioned, the code section plays a key role while keeping in mind the aspects of the theory. Current and power monitoring are shown in Figures 8 and 9. In brief, the initial section of code handles the microcontroller (ESP32) libraries, which include support for the device's Xtensa 32-bit dual-core microprocessor, 4 MB of flash memory, 520 Kb of SRAM, and a variety of communication protocols and interfaces [5]. Our gadget uses Wi-Fi, a wireless networking standard compliant with IEEE 802.11 b/g/n. The Wi-Fi connection is set up with the appropriate baud rate and variables are initialised. Wi-Fi can be connected in three different ways: through a station, an access point, or both [1]. To facilitate data uploads to the cloud, the device initially launched in STA+AP mode, which allows mobile devices to connect and relay the SSID and password of the router/hotspot that is connected to the Internet. The ADC reads data from the pin and sends it to a defined function that performs weighted and relative computations based on the ADC's resolution. For convenience in processing, a calibration factor is defined after the calculation algorithm.

Different criteria are imposed on the current value with decisions/outputs driving the result. The final output is data written to a designated area of the cloud (ThingSpeak, the Google Cloud Platform, and Amazon Web Services). Data are processed with a variety of statistical operations in the cloud to generate a consumption histogram and then compressed for storage. The equivalent instantaneous inductance (EII)-based technique [16], based on the theory of inductance, has been used to distinguish between inrush current and fault current in transformers. The EII varies greatly with inrush current but remains relatively constant with faulty phase. Consecutive current levels above a particular jump are compared, and if they fluctuate, this is interpreted as an inrush or fault current, setting off relays. Figure 10 shows the inrush and fault current graphs.



Figure 8. Block flow diagram.

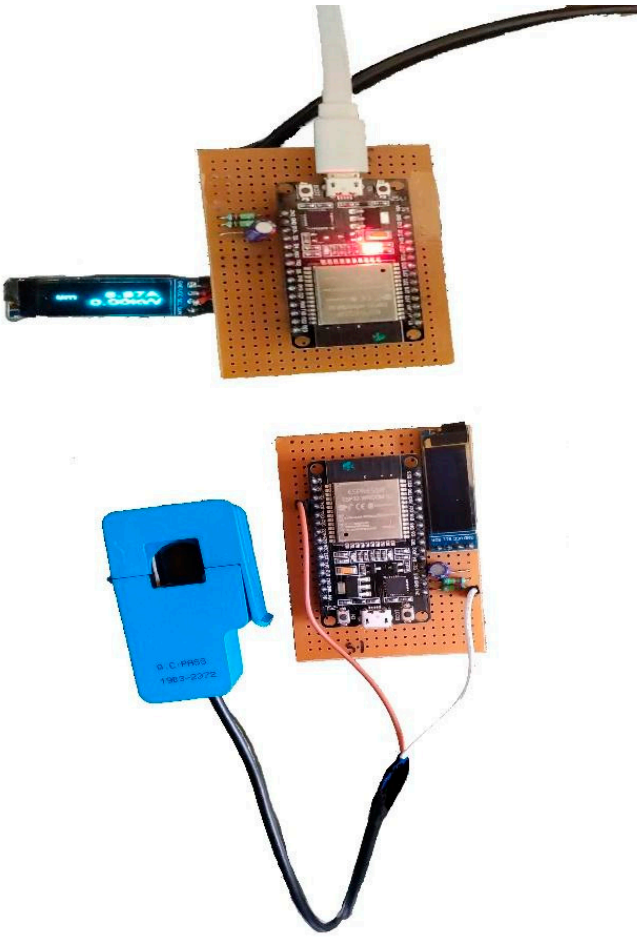


Figure 9. Current and power monitor.

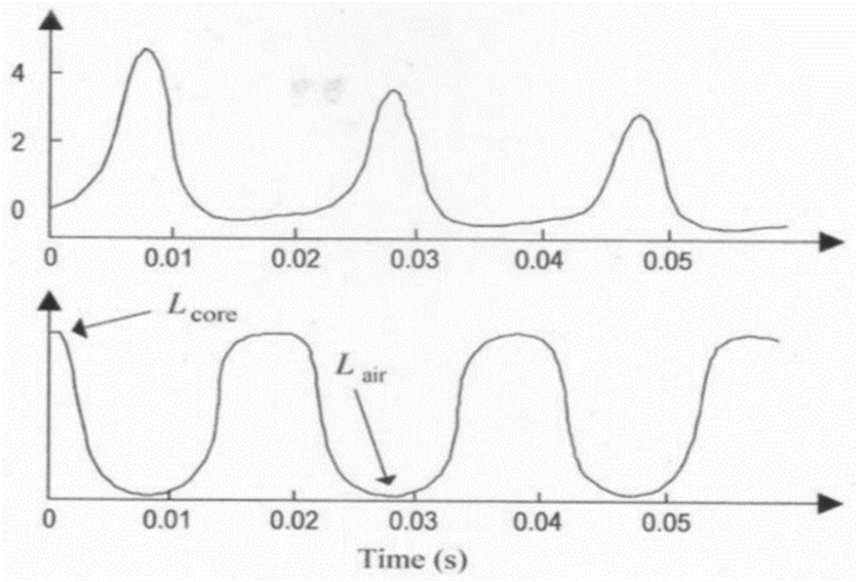


Figure 10. Inrush and fault current graphs [16].

7. Conclusions

Existing energy metering solutions are intricate, requiring professionals for installation, maintenance, and submetering due to their reliance on electromagnetic ideas and moving parts. Easy-to-use, low-cost, and remotely monitored power/current measurement devices are required for widespread adoption of metering in order to resolve power loss and power theft and ensure safety. Our clamp-on device's secondary half communicates with the microcontroller ESP32, which determines the current in the primary wire, to produce a signal proportionate to the primary current. Existing metering devices have their own set of challenges, but this new system can accurately estimate power consumption, prevent theft, and reduce power shortages and wastage due to overgeneration, all while displaying the current value and the amount of power used on an OLED display, which is uploaded to the cloud. This low-cost yet powerful tool may address a wide range of submetering and metering requirements, as well as offer a portable monitoring solution.

8. Future Work

This model might be greatly enhanced by using a higher-resolution ADC or tailoring the amplification of the signal. Measuring the phase difference in terms of time between successive peaks of voltage and current is an accurate way to compute true/real power and reactive power in addition to the RMS values of voltage and current. The above-described load characteristics and voltage and current waveforms [11] can be constructed to better understand the consumption/load pattern. The development phase is also a good time to implement push alerts to alert users of any connectivity or functionality issues with their devices. Industry uses include supporting the Industrial Internet of Things (IIOT) and providing safety for heavy machinery from the command control centre wirelessly, and the data can be used in real-time by higher levels, enabling the speedy resolution of faults or modifications to be made. By increasing the CT's resolution, we may draw more precise voltage, current, and power curves at more advanced programming levels using precise values from the ADC to the microcontroller, despite experiencing larger variance in the top band of measurements. Perfect graphs are generated by amplifying the signals and filtering out the noise. The scope of this model can be increased by adding certain Texas Instrument chips and Intel processors, albeit doing so may be too expensive for most people. If enough time and energy are put in, however, the quantity of resolve will be astounding. This device excels in measuring the energy use of large buildings, factories, and even farms. Along with the device's ultra-low power consumption mode, energy harvester pathways can be designed for the module. Infinite improvements to this method could be made.

Author Contributions: Conceptualisation, A.C.; methodology, A.C.; software, A.C.; validation, A.G.; formal analysis, A.G.; investigation, A.G.; resources, A.C.; data curation, A.C.; writing—original draft preparation, A.C.; writing—review and editing, A.G.; visualisation, A.G.; supervision, A.G.; project administration, A.G. All authors have read and agreed to the published version of the manuscript.

Funding: This research received no external funding.

Institutional Review Board Statement: Not applicable.

Informed Consent Statement: Not applicable.

Data Availability Statement: Data are contained within the article.

Conflicts of Interest: The authors declare no conflicts of interest.

References

1. Hoddie, P.; Prader, L. *IoT Development for ESP32 and ESP8266 with JavaScript: A Practical Guide to XS and the Moddable SDK*; Apress: Berkeley, CA, USA, 2020.
2. Viciana, E.; Arrabal-Campos, F.M.; Alcayde, A.; Baños, R.; Montoya, F.G. All-in-one three-phase smart meter and power quality analyzer with extended IoT capabilities. *Measurement* **2023**, *206*, 112309. [CrossRef]
3. Sen, V.; Dimothe, V. Perception towards time of use (TOU) electricity pricing amongst residential consumers in Maharashtra. In Proceedings of the AIP Conference Proceedings, Provo, UT, USA, 16–21 July 2017; AIP Publishing LLC: Melville, NY, USA, 2023; Volume 2523, p. 030009.
4. Kirmani, S.; Mazid, A.; Khan, I.A.; Abid, M. A Survey on IoT-Enabled Smart Grids: Technologies, Architectures, Applications, and Challenges. *Sustainability* **2023**, *15*, 717.
5. Belsare, K.; Rodriguez, A.C.; Sánchez, P.G.; Hierro, J.; Kołcon, T.; Lange, R.; Lütkebohle, I.; Malki, A.; Losa, J.M.; Melendez, F.; et al. Micro-ROS. In *Robot Operating System (ROS) the Complete Reference*; Springer International Publishing: Cham, Switzerland, 2023; Volume 7, pp. 3–55.
6. Campbell, B.; Dutta, P. Gemini: A non-invasive, energy-harvesting true power meter. In Proceedings of the 2014 IEEE Real-Time Systems Symposium, Rome, Italy, 2–5 December 2014; IEEE: Piscataway, NJ, USA, 2014; pp. 324–333.
7. Haghani, S.; Rahimi, M.A. The design and Implementation of a Smart Switch Outlet Adapter. In Proceedings of the 2018 ASEE Mid-Atlantic Section Spring Conference, Washington, DC, USA, 6–7 April 2018.
8. Yan, W.; Ma, C.; Cai, X.; Sun, Y.; Zhang, G.; Song, W. Self-powered and wireless physiological monitoring system with integrated power supply and sensors. *Nano Energy* **2023**, *108*, 108203.
9. Australian Energy Statistics. Australian Energy Update. In *Department of the Environment and Energy*; Commonwealth of Australia Canberra: Canberra, Australia, 2019; p. 36.
10. DeBruin, S.; Ghena, B.; Kuo, Y.-S.; Dutta, P. Powerblade: A low-profile, true-power, plug-through energy meter. In Proceedings of the 13th ACM Conference on Embedded Networked Sensor Systems, Seoul, Republic of Korea, 1–4 November 2015; pp. 17–29.
11. Stusek, M.; Pokorny, J.; Masek, P.; Hajny, J.; Hosek, J. A non-invasive electricity measurement within the smart grid landscape: Arduino-based visualization platform for IoT. In Proceedings of the 2017 9th International Congress on Ultra Modern Telecommunications and Control Systems and Workshops (ICUMT), Munich, Germany, 6–8 November 2017; IEEE: Piscataway, NJ, USA, 2017; pp. 423–429.
12. Quindai, R.; Almeida, C.M.P.; Ramos, H.S.; Rodrigues, J.J.P.; Aquino, A.L.L. A non intrusive low cost arduino-based three phase sensor kit for electric power measuring. In Proceedings of the 2017 2nd International Multidisciplinary Conference on Computer and Energy Science (SpliTech), Split, Croatia, 12–14 July 2017; IEEE: Piscataway, NJ, USA, 2017; pp. 1–6.
13. Xu, Q.R.; Paprotny, I.; Seidel, M.; White, R.M.; Wright, P.K. Stick-on piezoelectromagnetic AC current monitoring of circuit breaker panels. *IEEE Sens. J.* **2012**, *13*, 1055–1064. [CrossRef]
14. Geng, G.; Yang, X.; Gao, Y.; Hammond, W.; Xu, W. Noninvasive current sensor for multicore cables. *IEEE Trans. Power Deliv.* **2018**, *33*, 2335–2343. [CrossRef]
15. Wille, K.F.; Fitzgibbon, K. Non-invasive current measurement pulsed electron system and measurement techniques. In Proceedings of the IEEE AUTOTESTCON, Huntsville, AL, USA, 17 October 2002; IEEE: Piscataway, NJ, USA, 2002; pp. 541–550.
16. Sinha, A.; Kaur, S. Different Methods of Differentiating Inrush Current from Internal Fault Current in Transformer. *Int. J. Comput. Appl.* **2016**, *975*, 8887.
17. Al-Turjman, F.; Abujubbeh, M. IoT-enabled smart grid via SM: An overview. *Future Gener. Comput. Syst.* **2019**, *96*, 579–590. [CrossRef]
18. Goudarzi, A.; Ghayoor, F.; Waseem, M.; Fahad, S.; Traore, I. A Survey on IoT-Enabled Smart Grids: Emerging, Applications, Challenges, and Outlook. *Energies* **2022**, *15*, 6984.
19. Fadlullah, Z.M.; Pathan, A.-S.K.; Singh, K. Smart grid internet of things. *Mob. Netw. Appl.* **2018**, *23*, 879–880.

20. Minh, Q.N.; Nguyen, V.-H.; Quy, V.K.; Ngoc, L.A.; Chehri, A.; Jeon, G. Edge Computing for IoT-Enabled Smart Grid: The Future of Energy. *Energies* **2022**, *15*, 6140.
21. Kabalci, Y.; Kabalci, E.; Padmanaban, S.; Holm-Nielsen, J.B.; Blaabjerg, F. Internet of things applications as energy internet in smart grids and smart environments. *Electronics* **2019**, *8*, 972. [CrossRef]

Disclaimer/Publisher's Note: The statements, opinions and data contained in all publications are solely those of the individual author(s) and contributor(s) and not of MDPI and/or the editor(s). MDPI and/or the editor(s) disclaim responsibility for any injury to people or property resulting from any ideas, methods, instructions or products referred to in the content.